
SRIFT: SWIFT AND THRIFT CLOUD-BASED DISTRIBUTED TRAINING

Liang Luo^{1,2} Peter West¹ Arvind Krishnamurthy¹ Luis Ceze^{1,3}

ABSTRACT

Cost-efficiency and training time are primary concerns in cloud-based distributed training today. With many VM configurations to choose from, *given a time constraint, what configuration achieves the lowest cost?* Or, *given a cost budget, which configuration leads to the highest throughput?* We present a comprehensive throughput and cost-efficiency study across a wide array of instance choices in the cloud. With the insights from this study, we build Srift, a system that combines runtime instrumentation and learned performance models to accurately predict training performance and find the best choice of VMs to improve throughput and lower cost while satisfying user constraints. With Pytorch and EC2, we show Srift’s choices of VM instances can lead to up to 2x better throughput and 1.6x lower cost per iteration compared to baseline choices across various DNN models in real-world scenarios, leveraging heterogeneous setups and spot instances.

1 INTRODUCTION

With server demand for distributed training workload increasing steadily (Naumov et al., 2020; Jouppi et al., 2017; Fowers et al., 2018; Xiao et al., 2018), distributed training has become an important workload in public clouds (Google; Tra; Amazon, b). To date, most efforts (Smith et al., 2017; Sun et al., 2019; Goyal et al., 2017; Luo et al., 2020; 2018b) focus on improving training throughput in datacenter and public cloud environments.

However, minimizing training time is not the only goal. Recently, the monetary cost of cloud-based training jobs has soared to millions of dollars (Beat, 2020; Review, 2019), making cost a critical concern (MLPerf, 2020; Amazon, 2020) that deserves more attention. But minimizing cost itself is not meaningful without taking training time into consideration. So, given a time constraint, what choice of VM instances minimizes the cost? Or, symmetrically, given a cost budget, which instances minimize training time?

These questions are hard to answer, requiring accurate estimations of training performance for potentially unseen DNN models in a large space of cloud-provided configurations (VM families, sizes, and quantities). Modern cloud infrastructures bring additional challenges: performance variation introduced by multi-tenancy and the dynamic nature of the traffic add difficulty to performance prediction; the volatile availability and price of computing resources in public clouds may demand the use of heterogeneous configurations and spot instances to achieve objectives (§ 2).

Our work focuses on designing a system to find the best VM instances to train a DNN model in the cloud, given user objectives and constraints. Specifically, we address the

following challenges: first, we must understand both the temporal and spatial variation induced by the cloud environment, in terms of compute and communication performance; second, we must accurately estimate the training throughput of an unknown DNN model to derive the time and cost of executing the model with a particular choice of VMs, including heterogeneous setups; third, we must efficiently navigate the large search space to find the optimal choice and react to unexpected service interruptions if spot instances are used.

We propose Srift, a system that searches for the best VMs (potentially leveraging heterogeneous configurations and spot pricing) to lower training costs or improve throughput while satisfying user constraints. Srift draws insights from a comprehensive exploration of throughput and cost efficiency across different VMs on the public cloud (§ 3), and uses the following components to address the challenges above (§ 4): (1) an effective, instrumentation-based, DNN-agnostic mechanism to predict compute latency, taking into account variance from the cloud; (2) an empirically-learned communication bandwidth model based on various instance types and sizes across multiple regions in the public cloud; (3) a simulator to combine the models (1) and (2) by simulating the actual execution to derive a per-iteration latency; (4) an optimizer and a runtime that can efficiently search for the optimal solution, keep track of the current training progress, and react to service interruptions by searching again for new VM choices that can meet the original constraints.

We integrate Srift with Pytorch. On EC2, Srift achieves a training time and cost prediction error of 9% across various DNN models and VM setups and is able to find VM choices that lead to up to 2x better throughput with 1.6x lower cost/iteration in real-world training scenarios (§ 5).

2 CHALLENGES IN CLOUD-BASED DISTRIBUTED TRAINING

Distributed training has gained significant traction recently thanks to the introduction of effective large-batch optimization techniques (You et al., 2017; 2019b;a; Goyal et al., 2017), which allow larger global batch sizes and thus larger-scale distributed training to achieve equally good accuracy¹.

In this work, we focus on *synchronous data parallelism* due to its overwhelming popularity. Data parallelism distributes samples to different worker nodes, where the global batch size and other hyperparameters determine the outcome, regardless of how the global batch is distributed to workers. A batch of samples on a worker (per-device batch) experiences two phases (an iteration), a compute-intensive phase, followed by a parameter (gradient) exchange phase. Accurate estimation of the per-iteration time relies on good modeling of both. This work focuses on predicting per-iteration latency, a prerequisite for reliably predicting total training time and cost, as users often specify the number of iterations and epochs to train before checking the outcome.

Cloud environments add challenges to predicting iteration latency due to the unique infrastructures and dynamic, sharing nature.

2.1 The Compute Phase

The compute phase of an iteration consists of a forward and backward pass. In the forward pass, errors are computed; in the backward pass, gradients are derived. The compute phase is run independently on all accelerators.



Figure 1. Training iteration (ResNet18 @ batch size) latency varies from VM to VM on 64 p3 (top), g4dn (mid) and g3 (bottom) instances. Nodes are sorted based on their finish time. Darker-shaded nodes finish later than lighter-shaded node. The fast nodes are up to 1.2x faster than the slow ones.

Even with advanced pass-through techniques (Dong et al., 2012), shareable physical hardware cannot be made interference-free in the compute phase. We can observe both spatial variance (across different nodes) and temporal variance (across different iterations) of iteration time for the same workload. We run independent ResNet18 training tasks on 64 instances on EC2. Spatially, we color-code the per-VM iteration latency in heat maps shown in Figure 1:

¹Choosing the right batch size is beyond the scope of this work, and we assume the user has a target batch size in mind.

	p3.2xl	g3.4xl	g4dn.4xl
std/mean	5.2%	4.3%	6.7%

Table 1. Standard deviation over mean of compute-latency across 100 iterations on 3 instance types. Each averaged on 64 nodes.

	Rated	STD	Mean	Median	High	Low
p3.8xl	10	0.98	11.2	11.6	12.1	9.6
g3.8xl	10	0.31	11.9	11.8	12.2	7.1
g4dn.4xl	25*	0.74	20.3	20.3	25.4	20.3

Table 2. Pair-wise bandwidth (Gbps) probe results on 3 pairs of EC2 instances, averaged readings of every 10 seconds. * denotes a variable bandwidth.

the fastest node finishes more than 1.1x faster than the slowest node. Temporally, we summarize the standard deviation over the mean latency of 100 iterations in Table 1: there is a non-negligible difference across different iterations even on the same VM. These empirical findings challenge existing modeling techniques that are based only on static properties of the model and hardware spec (Qi et al., 2016; Pei et al., 2019; Justus et al., 2018; Cai et al., 2017) as they overestimate performance, because the slowest node straggles the training in a synchronous distributed setting.

2.2 The Parameter Exchange Phase

In synchronous distributed training, gradients are accumulated and averaged across all accelerators, known as parameter exchange. Modern frameworks overlap parameter exchange and backward pass (Justus et al., 2018; Zhang et al., 2017; Peng et al., 2019; Jayarajan et al., 2019; Hashemi et al., 2018): as gradients become available for each layer, they are processed without waiting for previous layers. A good model of the overlapping behavior requires exact timestamps of when a layer’s backward pass is finished. The main vehicles for parameter exchange are *parameter servers* (Smola & Narayanamurthy, 2010; Li et al., 2014a;b; Zhang & Ré, 2014; Luo et al., 2018a; Zhang et al., 2017; Cui et al., 2016) and *collective allreduce* (Sack, 2011; Thakur et al., 2005; Rabenseifner, 2004; Blum et al., 2000). We use collective allreduce in this work because it achieves better performance than parameter servers (Sergeev & Balso, 2018; Malik et al., 2018; Alqahtani & Demirbas, 2019).

Modern datacenter networks have a hierarchical, multi-tiered topology (Mysore et al., 2009; Greenberg et al., 2009; Roy et al., 2015; Liu et al., 2017). It is observed that the point-to-point communication performance of VMs varies greatly due to design choices (e.g., oversubscription (Bilal et al., 2012)), sharing (Luo et al., 2020), and cloud-specific mechanisms (e.g., credit-based (Amazon, c) fairness policy and bursting (Amazon, a) on EC2).

(Luo et al., 2020) quantifies volatile latency fluctuations between a pair of VMs, which directly impact latency-sensitive communications. To measure the degree of variation in

bandwidth, we run a 24-hour continuous bandwidth tracing with `iperf` for three pairs of different types of VMs in EC2. Table 2 summarizes the findings: in all traces, we observe bandwidth fluctuations and its deviation from the VM’s spec. This renders existing formula-based solutions that rely on a bandwidth rating from the cloud provider for estimating parameter exchange time such as (Qi et al., 2016; Zheng et al., 2019) ineffective as they can both under- or overestimate performance.

2.3 VM Selection

Cloud providers offer a large selection of VMs for running distributed training tasks: there are different families of VMs (with different accelerators such as GPU, CPU, FPGA (Fowers et al., 2018) and TPU (Jouppi et al., 2017)), each includes multiple generations, and within a generation, different sizes. On top of these, each VM can be billed as on-demand (uninterrupted, at a higher cost) or spot (can be preempted, with a lower cost) instances. Adding to the complexity, the user also needs to decide a per-device batch size, which corresponds to the number of instances to use given a global batch size. Sometimes, when the cloud is running out of resources, the request for VM instances cannot be fulfilled, and the alternative choices may include heterogeneous setups. All these factors create a large search space that makes the best configuration hard to find.

3 NAVIGATING THE COST-EFFICIENCY LANDSCAPE ON THE CLOUD

We present a comprehensive throughput and cost-efficiency (defined as throughput per hour-price) study on EC2 and Pytorch that helps us prune the search space. We use the following observation to help us prune the search space: *if an instance type has both lower throughput and lower cost-efficiency than another, then the former should not be considered.* In our study, we include four benchmarking models: ResNet50, an industry standard benchmark (Reddi et al., 2019); Vgg19, a compute- and communication-intensive model; SqueezeNet, a compute and communication-light model; and AlexNet, a compute-light but communication-intensive model. To simplify explanation, we use on-demand price to compute cost-efficiency in this section, and report a single averaged cost-efficiency across four models. We experiment on 6 representative VM types in Table 3, including compute-optimized c5 CPU-only instances, and 3 current generations of GPU instances, g3, g4dn and p3, each with up to 32 instances. For GPU instances, we use a per-device batch size that saturates both the compute and memory capacities, and for the CPU instances, we saturate the compute capacity. We use NCCL (Jeaugey, 2017) and Gloo (fac, 2020) as the communication backends.

	p3.2xl	p3.8xl	g3.4xl	g4dn.4xl	c5.4xl	c5.18xl
Acc.	V100	4V100	M60	T4	36 cores	72 cores
Gbps.	10*	10	10*	25*	10*	25

Table 3. Hardware and network bandwidth (Gbps) spec of the instances used in our study.

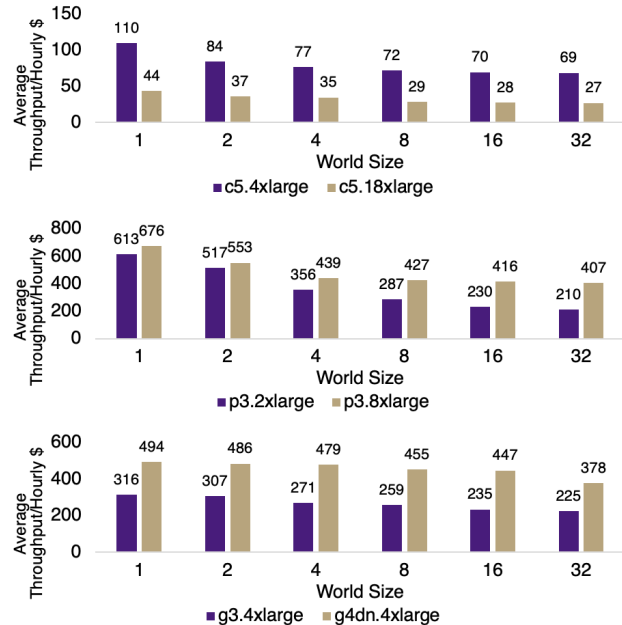


Figure 2. Average cost-efficiency across 4 different models on CPU and GPU instances of varying instance sizes and world sizes (weak scaling).

3.1 GPU vs CPU Instances

CPUs are not up to the task of DNN training when it comes to throughput. But can they provide an attractive cost-efficiency? Unfortunately, based on current pricing, CPUs are still not the best deal: as shown in Figure 2 (top and mid), even the less cost-efficient instances in the p3 family are 3x better than the more cost-efficient instances in the c5 family. In fact, this observation holds true when comparing other families of GPU instances (g3, g4dn). Thus, we should choose GPU instances whenever possible.

3.2 Older vs. Newer Generation of Instances

No universal conclusion on generation preference can be drawn from our study based on the current throughput and pricing for different generations of GPU instances: g3, p3, and g4dn instances are equipped with three different generations of GPUs, but they are not strictly getting more powerful nor cost-efficient: p3 (Tesla V100) has the highest throughput, but g4dn (Tesla T4) has better cost-efficiency, as shown in Figure 2 (bottom). We should not prune search space based on generation.

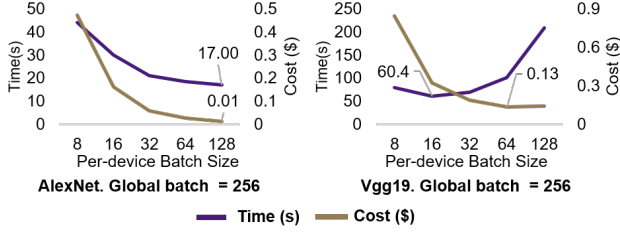


Figure 3. No magic batch size achieves the best throughput or lowest cost for all models, given a global batch size (strong scaling).

3.3 Smaller vs Larger Instances

How does cost-efficiency change with the size of VM in the same family? We compare different sizes of VMs in c5 and p3 families. Since VMs are priced up proportionally with their compute capacity, with ideal vertical scaling, cost-efficiency should be constant. In reality, c5 throughput scales poorly with added CPU cores, likely due to OpenMP overhead; on the other hand, larger p3 instances achieve better cost-efficiency due to the near-linear scaling of throughput with added GPUs and fast GPU interconnects. Thus, we prefer larger GPU instances but not larger CPU instances.

3.4 Horizontal Scalability

Practitioners use two main approaches to parallelize training, *weak scaling* (Figure 2), where accelerators use a “magic number” for batch size (e.g., 32 (StackExchange)), or *strong scaling* (Figure 3), where a fixed global batch size is chosen, and accelerators receive equal shards (Keras, 2020).

While all instances suffer from decay in cost-efficiency with larger world size, the best VM choice needs to be decided case by case. For example, with weak scaling, if training with a single node then a p3.8xlarge instance is the most ideal. However, with 16 nodes, g4dn.4xlarge VMs strike a better deal thanks to their faster network. With strong scaling, finding the right amount of instances to distribute workload is crucial. Figure 3 plots the performance for different node counts given a global batch size and illustrates that there are significant implications on both throughput (up to 2.7x) and cost (up to 47x) when training selected DNNs. We must consider all factors to find the best option to horizontally scale training, and no one-size-fits-all choice for per-device batch size that achieves optimal throughput or cost-efficiency.

4 DESIGN & IMPLEMENTATION OF SRIFT

We now describe Srift, a system that lowers costs and improves training throughput by finding the best VM choices, taking into account user constraints. Based on our findings in § 2 and § 3, Srift must be able to:

- Estimate forward and backward pass time given an accel-

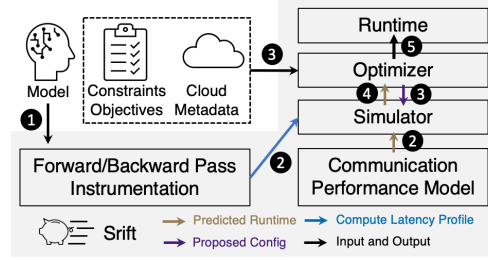


Figure 4. An overview of the Srift recommendation process. (1) user supplies a model, constraints and a goal; (2) Srift initializes the simulator with the compute and allreduce bandwidth models; (3-4) the Srift optimizer searches for the best configuration, using the predicted per-iteration runtime by the simulator; (5) Srift keeps track of training progress and suggests new configurations when service interruption occurs.

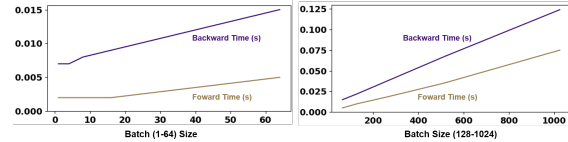


Figure 5. Forward and backward pass latency (AlexNet) exhibits a piece-wise linear relationship with per-device batch size.

- erator and a per-device batch size;
- Predict achieved communication bandwidth given the number of participating workers and buffer size;
- Take advantage of spot instance and heterogeneity;
- Dynamically adjust configuration to continuously optimize the objective in case of interrupts.

Srift uses following inputs to compute an ideal VM choice:

- User time and budget constraints, and an objective;
- Compute iteration latency profiles, built automatically *once per DNN per accelerator* with instrumentation;
- Allreduce bandwidth models, learned *once per cloud*.

Srift then feeds the inputs to a simulator to predict iteration latency given a VM choice, and searches through all possible VM choices to find the best choice for the objective, given the current availability, represented as two arrays: *counts*, *batches*. *counts[i]* is the number of *i*th instance-type of VM to launch, and *batches[i]* corresponds to the total batch size allocated to each VM of *i*th instance type. Figure 4 provides an overview.

4.1 Modeling Execution Time of Forward and Backward Passes

It is known that the forward and backward pass runtime t can be modeled with a linear relation (Crankshaw et al., 2017; Shen et al., 2019): given a device batch size B ,

$$t(B) = \alpha B + \beta \quad (1)$$

While the linear model fits well as a whole, we make a small change, using a piece-wise linear model to better capture smaller batch size time measurements (Figure 5), which generally have a different slope from larger batch sizes.

Srift starts by binary searching the maximum batch size B_{max} that can fit on a device, and samples forward and backward latency at four batch sizes: $1, \frac{1}{3}B_{max}, \frac{2}{3}B_{max}, B_{max}$, and use these points to create a 3-segment linear model. Srift sets up instrumentation hooks (Pytorch, 2020a; Tensorflow, 2020) to record the timestamp at which a particular layer (module) finishes backpropagation since the beginning of the backward pass. Capturing the timestamps allows Srift to accurately model the overlap of parameter exchanges later. Timestamps are normalized over the total backward pass time to allow extrapolation to different batch sizes.

Srift is topology- and structure-agnostic compared to other approaches that require detailed knowledge of the network such as (Qi et al., 2016). For networks that have parallel operations such as Inception, Srift naturally records the availability timestamps of the layers in the order of actual execution. Srift gives special care to dynamic networks that have conditional branches by sampling the dataset, and computes the probability of a layer being executed.

Srift parallelizes profiling of a DNN model for all available models of GPUs on the cloud, by launching multiple VMs. This process is done only once for a given model.

4.2 Estimating Allreduce Bandwidth

Estimating cloud-based communication performance is complex. The user has no visibility or control of the placement of VMs, making it difficult to derive a mathematical model. Further, end-to-end learning of parameter exchange time t given a model and number of participants (n , known as the world size) is difficult due to the fact that gradient transfers may overlap, and learning t for all possible ways of overlapping will be impractically costly in the public cloud.

Instead, Srift chooses to learn an alternative objective, the *bus bandwidth*, independently for different gradient size s . *Bus bandwidth* achieved during allreduce operation for gradient of size s is defined as $b_{bus} = \frac{2s(n-1)}{nt}$, and has an intuitive meaning: the average bandwidth to communicate a node’s shard of the parameter space to $n - 1$ other nodes, as physically measured from a network interface². Bus bandwidth also reduces aliasing of different setups into the same label: allreduce operations on different s may take the same time to finish if network transfer is dominated by network latency (e.g., $s \leq 1$ MTU), but they have different b_{bus} .

²Compared to *algorithm bandwidth* $b_{algo} = \frac{s}{t}$, bus bandwidth naturally incorporates world size n , and connects itself much closer to the actual physical hardware properties.

Srift performs a grid probe of allreduce bandwidth, by growing the buffer size from 4B to 512MB in a geometric sequence with powers of 2, and world size from 2 to 64 on g3, g4dn, and p3 instance families of different sizes on EC2. We warm up each probe to reduce variance due to bursting and interference. We include the following handpicked features in our dataset: location (cloud, region, and availability zone), GPU and CPU product name, CPU core count, memory size, rated network throughput (Gbps) by the provider, size of the buffer, the number of participants, and the number of asynchronous transfers. Our dataset contains 40K entries, in both EC2’s us-west-2 and us-east-1 regions. We repeat experiments multiple times, with potentially different VM spawns (reallocating) to capture variance induced by physical placement.

We use XGBoost (Chen et al., 2015) to train GBDT regression models. We find that the models predict negative bandwidth for small buffers when trained on the entire dataset, causing large test error. We mitigate this by training different models on two halves of the dataset, one for $s \leq MTU$, and one for $s \geq MTU$, where MTU is the maximum bytes a single network packet can carry (9K on EC2). This aligns with our domain knowledge that communication is latency bound for small buffers and bandwidth bound for large buffers. We perform model selection based on an auto-tuner and mean absolute percentage error (MAPE), sweeping various hyperparameters, such as objectives including pseudo huber loss (Huber, 1992), which is known to help with outliers. We find pseudo huber loss and squared error best minimizes MAPE for small and large transfer models, respectively. § 5.3 provides details of our final models.

Many frameworks use a dynamic scheme to switch among allreduce implementations based on transfer characteristics (e.g., NCCL switches between allreduce ring chunked and double binary tree algorithm). Our grid probe captures this.

4.3 Simulating Execution of an Iteration

The simulator outputs the predicted mean iteration latency for DNN model M : $t_{iter} = SIM(M, counts, batches, iters)$, with the help of the compute and allreduce bandwidth models.

A training iteration with batch size B would take $t_{iter} = t_{fw}(B) + \max(t_{bw}(B), t_{pe})$ to finish, where t_{fw} and t_{bw} are forward and backward pass times, and t_{pe} is the time for all layers to finish parameter exchange. We showed how to derive t_{fw} and t_{bw} . Since a selection of VMs (all instances i with $counts[i] > 0$) can contain heterogeneous hardware, the computation time is determined by the instance that takes the most time to finish the compute phase.

Srift considers stragglers when simulating the compute phase: each selected VM sample $iter$ values from a normal

distribution with a mean equal to the raw compute-latency prediction and a scale set to the empirical observation³. The max sampled value in each iteration becomes the predicted latency for that iteration, because the straggler determines execution time in a synchronous training setting. The mean iteration compute latency is then determined by averaging the predicted latency for all *iters* iterations.

Once the mean iteration compute latency is determined, we use the allreduce bandwidth model to derive t_{ps} through a simulation. The simulation starts at timestamp 0, which is the beginning of the backward pass. The simulator contains an event queue ordered by timestamp: for each trainable layer in the neural network, an event of (start, timestamp) is queued, where timestamp is collected through the instrumentation of the backward pass.

Events are continuously dequeued by timestamp order, and *timespan* represents the duration between current timestamp and that of the previous event. When a start event is dequeued, the allreduce operation on that layer starts, and a concurrency counter c is incremented. The simulator queries the allreduce bandwidth model for the bus bandwidth b_{bus} for this layer of size s . Since our performance model is trained on a dataset that only has s that is a power of 2, binned to maximum of 256 intervals (XGBoost default), we round s up to the nearest power of 2 when querying performance. We then add the returned b_{bus} to an aggregate bandwidth counter b_{agg} . Since an instance has a limited total bus bandwidth b_{cap} , the simulator allocates total bandwidth equally to each transfer fairly:

$$b_{bus} = \begin{cases} b_{bus} & \text{if } b_{agg} < b_{cap} \\ \mathbf{min}(b_{bus}, \frac{b_{cap}}{c}) & \text{otherwise} \end{cases} \quad (2)$$

The simulator computes a finish time for a layer based on the current bus bandwidth allocated to that layer, and a (estimatedFinish, timestamp) event is queued. Whenever an event is processed, the simulator updates the estimated finish time by *timespan*. If the resulting event causes any transfer’s bandwidth to change, all active operations’ estimated finish time is recomputed, and new events are queued to reflect such change. The simulation finishes when no event is present in the queue, and the last processed timestamp marks the end of current iteration, which is t_{ps} .

For maximum compatibility, Srift’s simulator assumes no expert knowledge on the internals of the underlying framework (e.g., Pytorch bucketizes allreduce calls (Pytorch, 2020b)). Instead, Srift accurately models the case of ideal overlapping because modern frameworks are all highly optimized. However, the simulator can be easily extended to capture

³The scale is dependent on the instance type and DNN, and is computed during the profiling phase. Our study in § 2.2 on g3, g4dn, and p3 instances indicates a median scale of 3.6%.

specific framework optimizations if needed.

4.4 Optimizing the Objectives with Constraints

Srift’s optimizer finds the best configuration subject to a set of constraints. With DNN model M , target global batch size B_{global} , target number of iterations N and list of available instances $0 \dots I$ (spot or on-demand), their availability $CAPS[]$ and prices $P[]$, subject to a time constraint T_{lim} and monetary budget $\$_{lim}$, Srift optimizer finds the best configuration that minimizes:

$$Nt_{iter} \sum_{i \text{ in } I} (counts[i]P[i]) \quad \mathbf{or} \quad Nt_{iter}$$

subject to

$$\begin{aligned} B_{global} &= \sum_{i \text{ in } I} batches[i]counts[i] \\ \forall i \text{ in } I \quad counts[i] &\leq CAPS[i] \\ Nt_{iter} \leq T_{lim} \quad \mathbf{or} \quad Nt_{iter} \sum_{i \text{ in } I} (counts[i]P[i]) &\leq \$_{lim} \end{aligned}$$

This is a Bayesian optimization (Snoek et al., 2012) problem with the blackbox simulator routine *SIM*, and can be solved with a modern solver (Knudde et al., 2017). However, we leverage the following domain knowledge and insights from § 3 to efficiently enumerate the full search space: (1) $batches[i]$ is only up to a few thousand, usually a power of 2 on accelerators (StackOverflow; Intel), and should be large enough to saturate the hardware’s compute capacity; (2) in an optimal scheme, choosing an instance type implies all the instances of that type have the same batch size⁴; (3) if capacity allows, favor homogeneous to heterogeneous because heterogeneous VMs may have larger physical distances to each other, thus worse communication performance; (4) if capacity allows, favor a larger GPU instance over a smaller GPU instance, then over a CPU instance. We note that these are techniques for pruning the search space without compromising the optimality of the identified solution.

Srift can perform an efficient exhaustive search, which finishes quickly in practice because there are few GPU instance types in the existing cloud. When the search space is too big, Srift accelerates this process with an “eager” mode, a best-effort heuristic for determining some feasible solution within a solving time budget. It operates by *increasing heterogeneity on an instance-type-by-instance-type basis*: Srift ranks instances by preference (i.e., the best performing instances for either cost or time), then searches for desired selections by incrementally enabling choices for other instance types, returning the configuration that best satisfies

⁴Otherwise, equally distribute the total amount of samples to each instance of that type, and the new throughput is no worse.

the constraints within a solving time budget. For example, Srift checks if including only $K = 8$ (tunable parameter) instances of type 1 satisfies the constraint, before searching configurations including instance type 2. This heuristic intuitively reflects our goal to minimize heterogeneity.

Due to the large price discrepancy between on-demand and spot instances, Srift prefers spot instances to on-demand.

4.5 Monitoring and Reacting to Service Interruptions

Srift is designed to leverage spot instances to reduce cost, relying on cloud-specific mechanisms (e.g., saving disk volume (Amazon, 2017; Microsoft, 2020)) and framework model checkpoints to preserve training progress. Srift’s lightweight heartbeat detects when a spot instance is preempted, and can replenish the system with additional VM nodes if the interrupt may cause violation of the original user time constraints. Srift runtime instructs the live VM with the smallest rank to immediately perform a checkpoint, and terminate current training. When VMs are started, Srift runtime restarts the training task by having the VM broadcast the latest model⁵. Srift runtime keeps track of the current elapsed time t , cost c and iterations n finished. When recommending new VM instances, Srift reruns the optimizer with updated constraints of $N=n$, $\$_{lim}=c$, $T_{lim}=t$ and objectives. Srift, takes spot instance preemption as a signal of depletion of that instance type in the cloud’s idle pool, and will not choose that instance again. If the new constraints cannot be satisfied, the Srift runtime seeks further input from the user to abort or relax constraints.

5 EVALUATION

We now present a comprehensive evaluation of Srift. Our goals are: (1) measure the time and cost benefits of Srift with end-to-end training in real-world scenarios; (2) evaluate the end-to-end accuracy of Srift’s iteration time prediction as well as accuracy of the compute latency and allreduce performance models on varying configurations; (3) assess how well Srift runtime reacts to service interrupts.

5.1 Evaluation Setup

We evaluate Srift with Pytorch 1.5 and NCCL 2.4.8⁶, using Cuda 10.1 and CuDNN 7, on Linux kernel 5.3. We run our experiments on EC2’s g3, g4dn and p3 families of VMs (which are current generations of GPU-enabled instances).

In all experiments, we exclude script launch overhead, and

⁵Many frameworks perform the broadcast regardless at launch to synchronize the initial model.

⁶We modified the Pytorch script to accept different GPU counts on VMs to observe actual iteration latency. NCCL’s double binary tree algorithm hangs with some configurations in this case, and when it happens, we set it to use only the ring chunked algorithm.

	p3.8xl	g3.8xl	g4dn.2xl/8xl
AlexNet	8192	2048	2048
ResNet18	2048	512	512
ResNet50	512	64	64
Vgg19	512	64	128
ResNext50_32x4d	512	64	64
SqueezeNet1_1	2048	512	512
ShuffleNet_v2_x2_0	1024	256	256
Inception_v3	512	128	128
Hourly rate	\$3.68	\$0.69	\$0.72

Table 4. Spot price and max batch size supported by instances.

report average runtime performance over at least 100 iterations. Since Srift does not affect computation and thus has no impact on accuracy, we use throughput as our speedup metric. We ignore the once-per-DNN profiling time, and use a synthetic dataset that mimics the properties of ImageNet to remove data loading time, as it is not our focus and is usually hidden by the compute phase. We use fixed spot instance prices provided by EC2 throughout our experiments, as the prices do not change too frequently (Narayanan et al., 2020). We use 8 representative DNNs to evaluate Srift (Table 4). When reporting Srift’s prediction accuracy, we use mean absolute percentage error (MAPE) as our error metric.

5.2 End-to-end Time and Cost Benefit of Srift

We now demonstrate real-world time and cost improvements using Srift’s configurations over two static policies, the *cost-aware* policy (CAP) and the *throughput-aware* policy (TAP). CAP and TAP works by ranking the instances by their preference: CAP favors cheaper instances, and TAP favors faster ones. They then request instances in the rank order, until all samples are distributed (i.e., global batch size is allocated). Both CAP and TAP fully load GPUs with the maximum possible batch size (Table 4) to fully utilize compute resources. In each study, we show both the actual and predicted throughput and/or cost of configurations proposed by CAP, TAP and Srift. We assume Srift knows the amount of resources available at hand to simplify explanation. However, this is not necessary for Srift to operate (§ 4).

We use the format `<number><instance>@<batch>` to represent Srift selects `<number>` of instance type `instance`, each with a batch size of `batch`.

Case 1: minimize training time. 16 g4dn.8xlarge instances are available. Minimize training time of Inception with a global batch size of 1024, with infinite cost budget.

	Srift	CAP	TAP
Config	16g4dn@32	8g4dn@64	8g4dn@64
Pred. thru.	0.914s/iter	1.776s/iter	1.776s/iter
Actual thru.	0.876s/iter	1.774s/iter	1.774s/iter
MAPE	4.3%	0.1%	0.1%

Given that there is only one choice for the accelerator in this

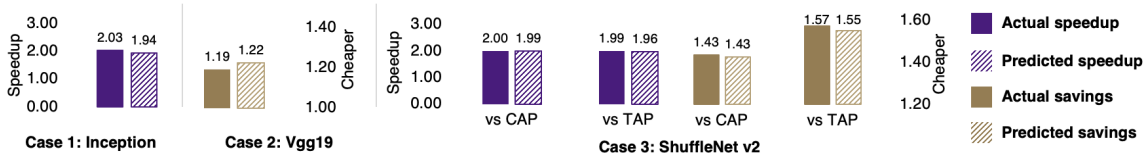


Figure 6. Swift accurately predicts throughput and costs. Swift’s choices reduce cost by up to 1.6x and improve throughput by up to 2x.

example, the optimization decision is to determine the per-device batch size and the corresponding number of devices. CAP and TAP use 8 g4dn instances. Swift proposes its choice of 16 g4dn accelerators within 0.67s, and predicts its choice is 1.94x faster than TAP and CAP’s. In reality, Swift’s configuration is 2.03x faster. Swift, by design, considers all configurations, so we also provide its prediction accuracies for the CAP and TAP configurations.

Case 2: minimize training cost. 16 instances each of g4dn.8xlarge and g3.8xlarge are available. Minimize training cost of vgg19 with a global batch size of 1024, assuming infinite time limit.

	Swift	CAP	TAP
Config	8g4dn@128	16g3@64	8g4dn@128
Pred. cost	\$0.321¢/iter	\$0.393¢/iter	\$0.321¢/iter
Actual cost	\$0.332¢/iter	\$0.396¢/iter	\$0.332¢/iter
MAPE	3.3%	0.7%	3.3%

Swift responds in 1.6s with the above configuration. It predicts its choice is 1.22x cheaper than CAP’s choice. In reality, Swift’s choice reduces cost by 1.19x.

Case 3: training with time and cost constraints. 4 p3.8xlarge, 8 g3.8xlarge and g4dn.8xlarge instances available. In last stages of layer-wise finetuning using gradual unfreezing (Griffiths, 2019; Howard & Ruder, 2018), train ShuffleNet for 1k iterations with a global batch size of 6K. Constraints: 10 minutes time and \$3 budget.

	Swift	CAP	TAP
Config	4p3@1024+ 8g3@128 + 8g4dn@128	2p3@1024+ 8g3@256+ 8g4dn@256	4p3@1024+ 8g4dn@256
Pred. time	378s	751s	742s
Actual time	381s	761s	759s
Pred. cost	\$2.72	\$3.88	\$4.22
Actual cost	\$2.74	\$3.93	\$4.31
MAPE	0.8%	1.3%	2.2%

Swift returns result in 0.76s with the above configuration. Swift’s choice is heterogeneous. Swift predicts its choice is 1.99x and 1.42x better than CAP in throughput and cost, and 1.96x and 1.55x better than TAP. In reality, the actual improvement for throughput and cost are 2x, 1.43x over CAP, and 1.99x, 1.57x over TAP. Further, Swift’s solution satisfies constraints with abundant headroom, but CAP/TAP’s

choices exceed both time limit and cost budget. Although Swift slightly underestimated the run time, its prediction of improvements remain highly accurate.

Summarized in Figure 6, we showed Swift’s practicality and effectiveness in three real-world scenarios. Swift’s suggested configurations can reduce cost by up to 1.6x and increase throughput by up to 2x, compared to TAP and CAP. Swift’s prediction error for both cost and throughput is on average 1.8% across these studies. One could argue that more sophisticated metrics such as sample per dollar (SPD) can provide potentially better results, however, here we claim the fundamental problems with these policies are: (1) they can only optimize the objective (time or budget) but is unaware of the constraints; (2) throughput itself is a function of batch size, and thus cannot be derived statically.

5.3 Ablation Study: Accuracy of Different Components in Swift’s Prediction Pipeline

This section independently evaluates prediction accuracy of the compute-latency model, the allreduce bandwidth model, and the simulator. We use 1 GPU/VM in this section.

Simulator: End-to-end accuracy. We start with the overall end-to-end accuracy of the simulator, which glues predictions from the compute performance and allreduce bandwidth models. We use the simulator to predict end-to-end training iteration time of all networks in Table 4 on g3.8xlarge, p3.8xlarge, g4dn.8xlarge and g4dn.2xlarge instances, across multiple regions (us-west-2, us-east-1 on EC2). For each configuration, we use various batch sizes (a small batch size of 1, a typical batch size of 64, a large batch size near the capacity of the chosen GPU), and different world sizes (from 2-64). The result is a multi-dimensional table with 740 entries. To report its accuracy comprehensively and succinctly, we summarize Swift’s accuracy and ability to generalize across 3 dimensions: different networks, different world size, and different instance types, including instances with variable network performance (g4dn.2xlarge).

We summarize the result in Table 5. Averaging across all experiments, Swift achieves a MAPE of 8.6%. While Swift does well when predicting training time overall, one error type is more serious than the other: when actual time is longer than predicted, Swift can violate user constraints. We

DNN model	End-to-end (E2E) MAPE
AlexNet	11.1%
ResNet18	7.7%
ResNet50	7.6%
Vgg19	11.1%
ResNext50_32x4d	9.4%
SqueezeNet1_1	10.7%
ShuffleNet_v2_x2.0	6.0%
Inception_v3	7.7%

Instance	E2E MAPE
g3.8xl	8.0 %
p3.8xl	8.6 %
g4dn.8xl	9.3 %
g4dn.2xl	10.1 %

World size	E2E MAPE
2	8.8%
4	8.6%
8	7.5%
16	8.6%
32	8.1%
64	10.7%

Table 5. MAPE of end-to-end prediction aggregated by DNN (top), by instance type (bottom left) and by world size (bottom right). Average: 8.9%.

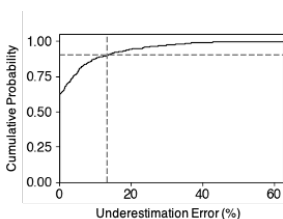


Figure 7. Cumulative distribution of underestimation error. Dotted line: 90% of the time underestimation error falls within 13.5%.

quantify this in Figure 7. In 61.3% of the cases Srift does not underestimate, and in 90% of the cases, Srift underestimates by no more than 13.5%. This demonstrates the robustness of Srift to outliers, and shows empirically Srift is unlikely to significantly violate user constraints⁷. Our further analysis shows that most error comes from the following setups: g4dn.2xlarge, as it has a variable bandwidth; AlexNet, Vgg and SqueezeNet, as they are communication latency or bandwidth sensitive and are more subject to cloud noise. Our prediction error also exhibits a “long tail”, coming from training runs with per-device batch size set to 1, which turns the training phase into a latency-bound process and drastically desynchronizes the nodes, causing larger relative errors in the prediction. Luckily, training with per-device batch size of 1 is rarely practiced in reality⁸.

Compute-latency Prediction Accuracy. We evaluate the compute-latency model on all networks in Table 4, by varying GPU (Tesla M60, Tesla T4, Tesla V100) and sweeping batch sizes from 1 to maximum in a geometric sequence

⁷Srift’s goal is to approximate training performance as accurate as possible, not minimizing underestimation error, because Srift can always choose to overestimate, but it renders Srift useless.

⁸As a side note, Srift’s prediction error is lowered to 6.3% if we exclude setups with per-device batch size of 1.

Network	Forward	Backward	Forward + Backward
AlexNet	8.0%	4.5%	3.9%
ResNet18	7.7%	3.9%	3.1%
ResNet50	5.6%	4.0%	3.0%
Vgg19	9.8%	3.0%	3.6%
ResNext50	5.5%	2.3%	2.4%
SqueezeNet	6.5%	9.5%	5.1%
ShuffleNet	10.1%	8.6%	8.0%
Inception	4.6%	6.8%	5.4%

GPU	Forward	Backward	Forward + Backward
Tesla M60	6.5%	3.3%	2.6%
Tesla T4	7.9%	5.2%	4.3%
Tesla V100	8.4%	7.9%	6.2%

Table 6. MAPE of compute latency model, aggregated by model (top) and aggregated by GPU (bottom).

with powers of 2. The results are summarized in Table 6. Overall, Srift’s compute-latency model achieves MAPE of 7.6%, 5.5%, 4.4% when predicting forward time, backward time, and the entire iteration time respectively.

Allreduce Bandwidth Model Accuracy. In order to understand the accuracy of the bandwidth model, we train with a stratified 9/1 train/test split. We tune hyperparameters by grid searching with a 10-fold cross-validation process. Our model achieves a MAPE of 11.7% on large transfers (buffer size larger than a MTU) and 23.9% on small transfers (buffer size no larger than a MTU) during test. As a comparison, if we simply used the rated bandwidth by the cloud provider as our prediction, the MAPE are at least 4000% for both small and large transfers, because transfer of small buffers can not fully utilize link bandwidth.

We now analyze the source of error. In our setup, each configuration (feature) is probed multiple times (reallocating VMs), giving different observations (labels). Since it is meaningless to produce a single aggregated observation due to unknown label distribution, no deterministic model can achieve a perfect error rate. In fact, our analysis shows a lower bound on error rate of 9.6% for small transfers and 8.2% for large. On one hand, this means that our model’s performance is close to the best achievable for large transfers; on the other hand, we are not concerned with the higher error rate on small transfers, because (1) they have little impact: they translate to only 10s of milliseconds of transfer time and can be hidden by the backward pass; (2) they are expected: physical affinity (VM allocation) has a higher impact on latency-bound transfers, as they are more sensitive to the noise in the cloud (Luo et al., 2020).

5.4 Reacting to Service Interruptions

We now evaluate how Srift’s runtime reacts to sudden interrupts during training due to spot instance preemption, by recomputing configurations that conform to updated constraints so the original constraints can be satisfied. In this section, we set some of the hyperparameters of Srift empiri-

cally: we expect EC2’s instance launch time to be 150s and EBS detach time to be 5s after an instance is terminated. We give Srift 1s solving time, and set its instance preference list to p3.8xlarge, g3.8xlarge then g4dn.8xlarge.



Figure 8. Srift dynamically changes recommended configuration to react to constraint changes due to service interrupts.

We train ResNet50 with a batch size of 1024 for 400 iterations, and we want it to finish within 500s, with a minimum cost. We provide no instance availability information to Srift. Srift incrementally solves the constraints by sequentially exploring more instance types and counts and returns the best configuration it can find within time limit. Srift starts with finding a candidate of 2 p3.8xlarge spot instances, each with 512 batch size. With this setup, the job is projected to finish in 152s (at time=302s, with 150s for launching instances). The instances finished launching at 138s.

When 200 iterations are finished, at time 222s, we cancel one spot instance to simulate a service interrupt. Srift detects the interrupt immediately, and starts working on an alternative configuration while EC2 makes the terminated instance’s volume ready, which takes 4s. Srift further needs to give EC2 150s in anticipation, to boot up an instance. Thus Srift must come up with a cost-efficient plan that finishes in 124s. Srift proposes to use an additional 8 g3.8xlarge (p3.8xlarge is not available) instances, each with a batch size of 64. The remaining 200 iterations are projected to finish in 100s, at 479s. It turns out the new 8 EC2 instances are able to boot in 95s. At time 419, training is completed. We summarize the observed key events in Figure 8: Srift is able to quickly react to service interrupts and use current progress to update constraints to propose a new configuration of instances, satisfying the original job’s constraints.

6 RELATED WORK AND DISCUSSION

Performance modeling. For forward pass performance modeling, (Qi et al., 2016; Pei et al., 2019) uses detailed knowledge of the DNN to estimate its computing latency, assuming peak accelerator performance and structural and topological information on the network are known, but peak performance is model dependent. (Cai et al., 2017) draws a correlation between parameter count and runtime. (Justus et al., 2018) trains a neural network to infer runtime. Srift improves on the linear model used in (Crankshaw et al., 2017; Shen et al., 2019; Qiao et al., 2020) to predict forward pass runtime. Srift achieves 3.9% MAPE compared to (Qi et al., 2016)’s 17% when estimating AlexNet’s compute

latency. For communication time modelling, (Zheng et al., 2019; Peng et al., 2018) consider only the parameter server architecture. (Qi et al., 2016; Peng et al., 2018; Zheng et al., 2019) relies on accurate bandwidth estimates. (Zheng et al., 2019) focuses on CPU instances only. Srift uses a learned-model that significantly lowered error compared to formula-based approaches that relies on an accurate, static bandwidth reading (He et al., 2005). For overlap modelling, (Zheng et al., 2019) assumes full overlap of both forward and backward passes, underestimating iteration time. (Qi et al., 2016; Peng et al., 2018) ignore overlap. (Qiao et al., 2020) learns an overlapping factor online during training. Srift collects detailed traces of when layer gradients become available to accurately determine overlapping.

Orthogonal to our work, (Jia et al., 2018; Mirhoseini et al., 2017) use RL to learn performance models. While effective, it can take hundreds of hours to finish for a single job on fixed hardware, which is prohibitively costly in the cloud.

Cost-awareness in cloud-based DNN training. (Zheng et al., 2019) focuses on predicting the optimal number of worker and parameter server nodes to minimize cost with a time constraint on CPU instances with fixed batch sizes, but does not deal with direct throughput constraints. (Narayanan et al., 2020) did an analytical study on how to leverage multiple clouds and spot pricing for training cost-reduction for specific DNNs. Elastic frameworks (Or et al., 2020) can improve cost-efficiency by adjusting training nodes with trial and error, by observing changes in the throughput, but they are best effort only and cannot deal with constraints directly, and does not assume optimality.

Predicting training time with loss curve. (Peng et al., 2018; Zheng et al., 2019) use loss curves to predict training time, assuming a smooth curve. Yet many models in trial and exploration phase (e.g., hyper-parameter tuning (Li et al., 2017; 2020)) may not convergence; some well established models (e.g. ResNet) can lack smooth curves (He et al., 2016; Gu et al., 2019). Thus, Srift does not use curve-fitting to predict training time, for more general use.

Beyond data parallelism. We mainly discuss data parallelism, but Srift does not rely on its specifics and can be applied to other paradigms. For example, Srift’s instrumentation of layer compute latency and communication performance model can predict training iteration time of model or pipeline parallelism by finding the slowest component.

7 CONCLUSION

Finding the best instances to meet a time or cost goal in cloud-based distributed training is difficult due to the large search space and unique challenges from the cloud environment. We presented Srift, an active training manager that draws insight from a comprehensive throughput and

cost-efficiency study to accurately predict training iteration time, and pinpoints the best instance configurations to reduce runtime and cost given constraints. We demonstrated Swift's benefit by improving throughput by up to 2x and reducing cost by up to 1.5x in real-world training scenarios in a public cloud.

REFERENCES

- Train and deploy machine learning models — microsoft azure. <https://azure.microsoft.com/en-us/free/machine-learning/>. (Accessed on 08/13/2020).
- facebookincubator/gloo: Collective communications library with various primitives for multi-machine training. <https://github.com/facebookincubator/gloo>, 08 2020. (Accessed on 08/24/2020).
- Alqahtani, S. and Demirbas, M. Performance analysis and comparison of distributed machine learning systems, 2019.
- Amazon. Benchmark network throughput between amazon ec2 linux instances in the same amazon vpc. <https://aws.amazon.com/premiumsupport/knowledge-center/network-throughput-benchmark-linux-ec2/>, a. (Accessed on 08/17/2020).
- Amazon. Deep learning on aws. <https://aws.amazon.com/deep-learning/>, b. (Accessed on 12/06/2018).
- Amazon. Memory optimized instances - amazon elastic compute cloud. <https://docs.aws.amazon.com/AWSEC2/latest/UserGuide/memory-optimized-instances.html#memory-instances-hardware>, c. (Accessed on 08/17/2020).
- Amazon. Amazon ec2 spot can now stop and start your spot instances. <https://aws.amazon.com/about-aws/whats-new/2017/09/amazon-ec2-spot-can-now-stop-and-start-your-spot-instances/#:~:text=To%20use%20this%20new%20feature,saved%2C%20and%20their%20data%20persists.,> 09 2017. (Accessed on 08/20/2020).
- Amazon. Amazon ec2 g4 instances — amazon web services (aws). <https://aws.amazon.com/ec2/instance-types/g4/>, 8 2020. (Accessed on 08/25/2020).
- Beat, V. Openai launches an api to commercialize its research — venturebeat. <https://venturebeat.com/2020/06/11/openai-launches-an-api-to-commercialize-its-research/>, 6 2020. (Accessed on 08/23/2020).
- Bilal, K., Khan, S. U., Kolodziej, J., Zhang, L., Hayat, K., Madani, S. A., Min-Allah, N., Wang, L., and Chen, D. A comparative study of data center network architectures. In *ECMS*, 2012.
- Blum, E. K., Wang, X., and Leung, P. Architectures and message-passing algorithms for cluster computing: Design and performance. *Parallel Computing*, 26(2-3):313–332, 2000.
- Cai, E., Juan, D.-C., Stamoulis, D., and Marculescu, D. Neuralpower: Predict and deploy energy-efficient convolutional neural networks, 2017.
- Chen, T., He, T., Benesty, M., Khotilovich, V., and Tang, Y. Xgboost: extreme gradient boosting. *R package version 0.4-2*, pp. 1–4, 2015.
- Crankshaw, D., Wang, X., Zhou, G., Franklin, M. J., Gonzalez, J. E., and Stoica, I. Clipper: A low-latency online prediction serving system. In *Proceedings of the 14th USENIX Conference on Networked Systems Design and Implementation*, NSDI'17, pp. 613–627, USA, 2017. USENIX Association. ISBN 9781931971379.
- Cui, H., Zhang, H., Ganger, G. R., Gibbons, P. B., and Xing, E. P. Geeps: Scalable deep learning on distributed gpus with a gpu-specialized parameter server. In *Proceedings of the Eleventh European Conference on Computer Systems*, pp. 4. ACM, 2016.
- Dong, Y., Yang, X., Li, J., Liao, G., Tian, K., and Guan, H. High performance network virtualization with sr-iov. *Journal of Parallel and Distributed Computing*, 72(11):1471–1480, 2012.
- Fowers, J., Ovtcharov, K., Papamichael, M., Massengill, T., Liu, M., Lo, D., Alkalay, S., Haselman, M., Adams, L., Ghandi, M., et al. A configurable cloud-scale dnn processor for real-time ai. In *Proceedings of the 45th Annual International Symposium on Computer Architecture*, pp. 1–14. IEEE Press, 2018.
- Google. Google cloud training. google cloud. <https://cloud.google.com/training/courses/machine-learning-tensorflow-gcp>. (Accessed on 03/04/2019).
- Goyal, P., Dollár, P., Girshick, R., Noordhuis, P., Wesolowski, L., Kyrola, A., Tulloch, A., Jia, Y., and He, K. Accurate, large minibatch SGD: Training ImageNet in 1 hour. *arXiv preprint arXiv:1706.02677*, 2017.

- Greenberg, A., Hamilton, J. R., Jain, N., Kandula, S., Lahiri, P., Maltz, D., and and. VI2: A scalable and flexible data center network. Association for Computing Machinery, Inc., August 2009. URL <https://www.microsoft.com/en-us/research/publication/vl2-a-scalable-and-flexible-data-center-network>. Recognized as one of "the most important research results published in CS in recent years".
- Griffiths, N. How to fine-tune your neural network for your data: Image classification — by nelson griffiths — towards data science. <https://towardsdatascience.com/how-to-fine-tune-your-neural-network-for-your-data-image-classification-d0f01c92300b>, 12 2019. (Accessed on 08/26/2020).
- Gu, J., Chowdhury, M., Shin, K. G., Zhu, Y., Jeon, M., Qian, J., Liu, H., and Guo, C. Tiresias: A {GPU} cluster manager for distributed deep learning. In 16th {USENIX} Symposium on Networked Systems Design and Implementation ({NSDI} 19), pp. 485–500, 2019.
- Hashemi, S. H., Jyothi, S. A., and Campbell, R. H. Tictac: Accelerating distributed deep learning with communication scheduling. arXiv preprint arXiv:1803.03288, 2018.
- He, K., Zhang, X., Ren, S., and Sun, J. Deep residual learning for image recognition. In 2016 IEEE Conference on Computer Vision and Pattern Recognition (CVPR), pp. 770–778, 2016.
- He, Q., Dovrolis, C., and Ammar, M. Prediction of tcp throughput: formula-based and history-based methods. volume 33, pp. 388–389, 01 2005.
- Howard, J. and Ruder, S. Universal language model fine-tuning for text classification, 2018.
- Huber, P. J. Robust estimation of a location parameter. In Breakthroughs in statistics, pp. 492–518. Springer, 1992.
- Intel. Cifar-10 classification using intel® optimization for tensorflow*. <https://software.intel.com/content/www/us/en/develop/articles/cifar-10-classification-using-intel-optimization-for-tensorflow.html>. (Accessed on 09/06/2020).
- Jayarajan, A., Wei, J., Gibson, G., Fedorova, A., and Pekhimenko, G. Priority-based parameter propagation for distributed dnn training. SysML 2019, 2019.
- Jeagey, S. Nccl 2.0. GTC, 2017.
- Jia, Z., Zaharia, M., and Aiken, A. Beyond data and model parallelism for deep neural networks. arXiv preprint arXiv:1807.05358, 2018.
- Jouppi, N. P., Young, C., Patil, N., Patterson, D., Agrawal, G., Bajwa, R., Bates, S., Bhatia, S., Boden, N., Borchers, A., Boyle, R., Cantin, P.-I., Chao, C., Clark, C., Coriell, J., Daley, M., Dau, M., Dean, J., Gelb, B., Ghaemmaghami, T. V., Gottipati, R., Gulland, W., Hagmann, R., Ho, C. R., Hogberg, D., Hu, J., Hundt, R., Hurt, D., Ibarz, J., Jaffey, A., Jaworski, A., Kaplan, A., Khaitan, H., Killebrew, D., Koch, A., Kumar, N., Lacy, S., Laudon, J., Law, J., Le, D., Leary, C., Liu, Z., Lucke, K., Lundin, A., MacKean, G., Maggiore, A., Mahony, M., Miller, K., Nagarajan, R., Narayanaswami, R., Ni, R., Nix, K., Norrie, T., Omernick, M., Penukonda, N., Phelps, A., Ross, J., Ross, M., Salek, A., Samadiani, E., Severn, C., Sizikov, G., Snellham, M., Souter, J., Steinberg, D., Swing, A., Tan, M., Thorson, G., Tian, B., Toma, H., Tuttle, E., Vasudevan, V., Walter, R., Wang, W., Wilcox, E., and Yoon, D. H. In-datacenter performance analysis of a tensor processing unit. In Proceedings of the 44th Annual International Symposium on Computer Architecture, ISCA '17, pp. 1–12, New York, NY, USA, 2017. ACM. ISBN 978-1-4503-4892-8. doi: 10.1145/3079856.3080246. URL <http://doi.acm.org/10.1145/3079856.3080246>.
- Justus, D., Brennan, J., Bonner, S., and McGough, A. S. Predicting the computational cost of deep learning models. In 2018 IEEE International Conference on Big Data (Big Data), pp. 3873–3882, 2018.
- Keras. Multi-gpu and distributed training. https://keras.io/guides/distributed_training/, 8 2020. (Accessed on 08/24/2020).
- Knudde, N., van der Herten, J., Dhaene, T., and Couckuyt, I. GPflowOpt: A Bayesian Optimization Library using TensorFlow. arXiv preprint – arXiv:1711.03845, 2017. URL <https://arxiv.org/abs/1711.03845>.
- Li, L., Jamieson, K., DeSalvo, G., Rostamizadeh, A., and Talwalkar, A. Hyperband: A novel bandit-based approach to hyperparameter optimization. The Journal of Machine Learning Research, 18(1):6765–6816, 2017.
- Li, L., Jamieson, K., Rostamizadeh, A., Gonina, E., Benztur, J., Hardt, M., Recht, B., and Talwalkar, A. A system for massively parallel hyperparameter tuning. In Proceedings of Machine Learning and Systems 2020, pp. 230–246. 2020.
- Li, M., Andersen, D. G., Park, J. W., Smola, A. J., Ahmed, A., Josifovski, V., Long, J., Shekita, E. J., and Su, B.-Y. Scaling distributed machine learning with the parameter server. In Proceedings of the 11th USENIX Conference on Operating Systems Design and Implementation, OSDI'14, pp. 583–598, Berkeley, CA, USA, 2014a. USENIX Association. ISBN 978-1-931971-16-4. URL <http://dl.acm.org/citation.cfm?id=2685048.2685095>.

- Li, M., Andersen, D. G., Smola, A., and Yu, K. Communication efficient distributed machine learning with the parameter server. In Proceedings of the 27th International Conference on Neural Information Processing Systems, NIPS'14, pp. 19–27, Cambridge, MA, USA, 2014b. MIT Press. URL <http://dl.acm.org/citation.cfm?id=2968826.2968829>.
- Liu, M., Luo, L., Nelson, J., Ceze, L., Krishnamurthy, A., and Atreya, K. IncBricks: Toward in-network computation with an in-network cache. SIGOPS Oper. Syst. Rev., 51(2):795–809, April 2017. ISSN 0163-5980. doi: 10.1145/3093315.3037731. URL <http://doi.acm.org/10.1145/3093315.3037731>.
- Luo, L., Nelson, J., Ceze, L., Phanishayee, A., and Krishnamurthy, A. Parameter hub: A rack-scale parameter server for distributed deep neural network training. In Proceedings of the ACM Symposium on Cloud Computing, SoCC '18, pp. 41–54, New York, NY, USA, 2018a. ACM. ISBN 978-1-4503-6011-1. doi: 10.1145/3267809.3267840. URL <http://doi.acm.org/10.1145/3267809.3267840>.
- Luo, L., Nelson, J., Ceze, L., Phanishayee, A., and Krishnamurthy, A. Parameter hub: a rack-scale parameter server for distributed deep neural network training. In Proceedings of the ACM Symposium on Cloud Computing, pp. 41–54, 2018b.
- Luo, L., West, P., Krishnamurthy, A., Ceze, L., and Nelson, J. Plink: Discovering and exploiting datacenter network locality for efficient cloud-based distributed training, 2020.
- Malik, A., Lu, M., Wang, N., Lin, Y., and Yoo, S. Detailed performance analysis of distributed tensorflow on a gpu cluster using deep learning algorithms. In 2018 New York Scientific Data Summit (NYSDS), pp. 1–8, 2018.
- Microsoft. Use azure spot vms - azure windows virtual machines — microsoft docs. <https://docs.microsoft.com/en-us/azure/virtual-machines/windows/spot-vms>, 07 2020. (Accessed on 08/20/2020).
- Mirhoseini, A., Pham, H., Le, Q. V., Steiner, B., Larsen, R., Zhou, Y., Kumar, N., Norouzi, M., Bengio, S., and Dean, J. Device placement optimization with reinforcement learning. arXiv preprint arXiv:1706.04972, 2017.
- MLPerf. How do mlperf v0.7 entries compare on cost? · stanford dawn. <https://dawn.cs.stanford.edu/2020/08/17/mlperf-v0.7-cost/>, 8 2020. (Accessed on 08/23/2020).
- Mysore, R. N., Pamboris, A., Farrington, N., Huang, N., Miri, P., Radhakrishnan, S., Subramanya, V., and Vahdat, A. Portland: a scalable fault-tolerant layer 2 data center network fabric. In SIGCOMM, 2009.
- Narayanan, D., Santhanam, K., Kazhemiaka, F., Phanishayee, A., and Zaharia, M. Analysis and exploitation of dynamic pricing in the public cloud for ml training. In DISPA 2020, 2020.
- Naumov, M., Kim, J., Mudigere, D., Sridharan, S., Wang, X., Zhao, W., Kim, C., Yuen, H., Ozdal, M., Nair, K., Gao, I., Su, B.-Y., Yang, J., and Smelyanskiy, M. Deep learning training in facebook data centers: Design of scale-up and scale-out systems, 03 2020.
- Or, A., Zhang, H., and Freedman, M. Resource elasticity in distributed deep learning. In MLSys, 2020.
- Pei, Z., Li, C., Qin, X., Chen, X., and Wei, G. Iteration time prediction for cnn in multi-gpu platform: Modeling and analysis. IEEE Access, 7:64788–64797, 2019.
- Peng, Y., Bao, Y., Chen, Y., Wu, C., and Guo, C. Optimus: an efficient dynamic resource scheduler for deep learning clusters. In Proceedings of the Thirteenth EuroSys Conference, pp. 1–14, 2018.
- Peng, Y., Zhu, Y., Chen, Y., Bao, Y., Yi, B., Lan, C., Wu, C., and Guo, C. A generic communication scheduler for distributed dnn training acceleration. In Proceedings of the 27th ACM Symposium on Operating Systems Principles, SOSP '19, pp. 16–29, New York, NY, USA, 2019. Association for Computing Machinery. ISBN 9781450368735. doi: 10.1145/3341301.3359642. URL <https://doi.org/10.1145/3341301.3359642>.
- Pytorch. nn package — pytorch tutorials 1.6.0 documentation. https://pytorch.org/tutorials/beginner/former_torchies/nnft_tutorial.html, 8 2020a. (Accessed on 08/18/2020).
- Pytorch. pytorch/_utils.py at be3ec6ab3e47736f03518537097815bc357f8ebe · pytorch/pytorch. https://github.com/pytorch/pytorch/blob/be3ec6ab3e47736f03518537097815bc357f8ebe/torch/_utils.py#L242, 9 2020b. (Accessed on 09/22/2020).
- Qi, H., Sparks, E. R., and Talwalkar, A. Paleo: A performance model for deep neural networks. 2016.
- Qiao, A., Neiswanger, W., Ho, Q., Zhang, H., Ganger, G. R., and Xing, E. P. Pollux: Co-adaptive cluster scheduling for goodput-optimized deep learning, 2020.

- Rabenseifner, R. Optimization of collective reduction operations. pp. 1–9, 06 2004. doi: 10.1007/978-3-540-24685-5_1.
- Reddi, V. J., Cheng, C., Kanter, D., Mattson, P., Schmuelling, G., Wu, C.-J., Anderson, B., Breughe, M., Charlebois, M., Chou, W., Chukka, R., Coleman, C., Davis, S., Deng, P., Damos, G., Duke, J., Fick, D., Gardner, J. S., Hubara, I., Ildgunji, S., Jablin, T. B., Jiao, J., John, T. S., Kanwar, P., Lee, D., Liao, J., Lokhmotov, A., Massa, F., Meng, P., Micikevicius, P., Osborne, C., Pekhimenko, G., Rajan, A. T. R., Sequeira, D., Sirasao, A., Sun, F., Tang, H., Thomson, M., Wei, F., Wu, E., Xu, L., Yamada, K., Yu, B., Yuan, G., Zhong, A., Zhang, P., and Zhou, Y. Mlperf inference benchmark, 2019.
- Review, S. The staggering cost of training sota ai models — synced. <https://syncedreview.com/2019/06/27/the-staggering-cost-of-training-sota-ai-models/#:~:text=The%20Register%20reports%20the%20GPT, costs%20US%24256%20per%20hour.,> 6 2019. (Accessed on 08/23/2020).
- Roy, A., Zeng, H., Bagga, J., Porter, G., and Snoeren, A. C. Inside the social network’s (datacenter) network. *Computer Communication Review*, 45:123–137, 2015.
- Sack, P. D. *Scalable Collective Message-passing Algorithms*. PhD thesis, Champaign, IL, USA, 2011. AAI3503864.
- Sergeev, A. and Balso, M. D. Horovod: fast and easy distributed deep learning in tensorflow, 2018.
- Shen, H., Chen, L., Jin, Y., Zhao, L., Kong, B., Philipose, M., Krishnamurthy, A., and Sundaram, R. Nexus: a gpu cluster engine for accelerating dnn-based video analysis. In *Proceedings of the 27th ACM Symposium on Operating Systems Principles*, pp. 322–337, 2019.
- Smith, S. L., Kindermans, P., and Le, Q. V. Don’t decay the learning rate, increase the batch size. *CoRR*, abs/1711.00489, 2017. URL <http://arxiv.org/abs/1711.00489>.
- Smola, A. and Narayanamurthy, S. An architecture for parallel topic models. *Proc. VLDB Endow.*, 3(1-2):703–710, September 2010. ISSN 2150-8097. doi: 10.14778/1920841.1920931. URL <http://dx.doi.org/10.14778/1920841.1920931>.
- Snoek, J., Larochelle, H., and Adams, R. P. Practical bayesian optimization of machine learning algorithms. In *Advances in neural information processing systems*, pp. 2951–2959, 2012.
- StackExchange. neural networks - how do i choose the optimal batch size? - artificial intelligence stack exchange. <https://ai.stackexchange.com/questions/8560/how-do-i-choose-the-optimal-batch-size>. (Accessed on 08/24/2020).
- StackOverflow. machine learning - what is the advantage of keeping batch size a power of 2? - data science stack exchange. <https://datascience.stackexchange.com/questions/20179/what-is-the-advantage-of-keeping-batch-size-a-pow>. (Accessed on 09/06/2020).
- Sun, P., Feng, W., Han, R., Yan, S., and Wen, Y. Optimizing network performance for distributed dnn training on gpu clusters: Imagenet/alexnet training in 1.5 minutes. *arXiv preprint arXiv:1902.06855*, 2019.
- Tensorflow. tf.registergradient — tensorflow core v2.3.0. https://www.tensorflow.org/api_docs/python/tf/RegisterGradient, 2020. (Accessed on 10/03/2020).
- Thakur, R., Rabenseifner, R., and Gropp, W. Optimization of collective communication operations in mpich. *Int. J. High Perform. Comput. Appl.*, 19(1):49–66, February 2005. ISSN 1094-3420. doi: 10.1177/1094342005051521. URL <http://dx.doi.org/10.1177/1094342005051521>.
- Xiao, W., Bhardwaj, R., Ramjee, R., Sivathanu, M., Kwatra, N., Han, Z., Patel, P., Peng, X., Zhao, H., Zhang, Q., Yang, F., and Zhou, L. Gandiva: Introspective cluster scheduling for deep learning. In *13th USENIX Symposium on Operating Systems Design and Implementation (OSDI 18)*, pp. 595–610, Carlsbad, CA, 2018. USENIX Association. ISBN 978-1-931971-47-8. URL <https://www.usenix.org/conference/osdi18/presentation/xiao>.
- You, Y., Gitman, I., and Ginsburg, B. Large batch training of convolutional networks, 2017.
- You, Y., Hseu, J., Ying, C., Demmel, J., Keutzer, K., and Hsieh, C.-J. Large-batch training for lstm and beyond. In *Proceedings of the International Conference for High Performance Computing, Networking, Storage and Analysis, SC ’19*, New York, NY, USA, 2019a. Association for Computing Machinery. ISBN 9781450362290. doi: 10.1145/3295500.3356137. URL <https://doi.org/10.1145/3295500.3356137>.
- You, Y., Li, J., Reddi, S., Hseu, J., Kumar, S., Bhojanapalli, S., Song, X., Demmel, J., Keutzer, K., and Hsieh, C.-J. Large batch optimization for deep learning: Training bert in 76 minutes. *arXiv preprint arXiv:1904.00962*, 2019b.

Zhang, C. and Ré, C. Dimm-witted: A study of main-memory statistical analytics. Proc. VLDB Endow., 7 (12):1283–1294, August 2014. ISSN 2150-8097. doi: 10.14778/2732977.2733001. URL <http://dx.doi.org/10.14778/2732977.2733001>.

Zhang, H., Zheng, Z., Xu, S., Dai, W., Ho, Q., Liang, X., Hu, Z., Wei, J., Xie, P., and Xing, E. P. Poseidon: An efficient communication architecture for distributed deep learning on GPU clusters. In 2017 USENIX Annual Technical Conference (USENIX ATC 17), pp. 181–193, Santa Clara, CA, 2017. USENIX Association. ISBN 978-1-931971-38-6. URL <https://www.usenix.org/conference/atc17/technical-sessions/presentation/zhang>.

Zheng, H., Xu, F., Chen, L., Zhou, Z., and Liu, F. Cynthia: Cost-efficient cloud resource provisioning for predictable distributed deep neural network training. In Proceedings of the 48th International Conference on Parallel Processing, pp. 1–11, 2019.